Clinical Oral Investigations (2021) 25:3589–3597
https://doi.org/10.1007/s00784-020-03681-y

ORIGINAL ARTICLE

Significance of implant design on the efficacy of different peri-implantitis decontamination protocols

Ignacio Sanz-Martín[1,2] · Kyeongwon Paeng[2] · Hyobin Park[2] · Jae-Kook Cha[2] · Ui-Won Jung[2] · Mariano Sanz[1,3]

Received: 22 July 2020 / Accepted: 4 November 2020 / Published online: 10 November 2020

Abstract

Objective To assess the efficacy of three mechanical decontamination methods in four types of commercially available implants.

Material and methods Ninety-six implants of four commercial brands with different designs (regarding thread depth and thread pitch) were soaked in a surrogate biofilm (ink) and air-dried. Circumferential standardized peri-implant defects with 6 mm in depth and 1.55 mm in width were custom-made with a 3D printer. Stained implants were inserted in the defects and instrumented with three different methods: a titanium brush (TNB), a metallic ultrasonic tip (IST) and an air abrasive (PF). Standardized photographs were taken vertically to the implant axis (flat view), and with angulations of 60° (upper view) and 120° (lower view) to the implant long axis. The percentage of residual stain (PRS) was calculated with the image analysis software. Scanning electron microscope evaluations were performed on the buccal aspect of the implants at the central level of the defect.

Results The efficacy of PF was significantly inferior to the TNB and IST in all implant designs, while there were no significant differences between TNB and IST. IST showed significantly higher PRS in the implant with the highest thread pitch, while the TNB had the highest PRS in the implant with a marked reverse buttress-thread design. The micro-thread design had the lowest values of PRS for all decontamination methods. The apically facing threads represented the areas with highest PRS for all implant designs and decontamination methods.

Conclusion Thread geometry influenced the access of the decontamination devices and in turn its efficacy. Implants with lower thread pitch and thread depth values appeared to have less residual staining.

Clinical relevance Clinicians must be aware of the importance of thread geometry in the decontamination efficacy.

Keywords Peri-implantitis · Surface decontamination · Dental implants · Scanning electron microscope · Implant design · Thread design

Introduction

Peri-implantitis has been recently defined as a plaque-associated pathological condition occurring in tissues around dental implants, characterized by mucosal inflammation in the peri-implant mucosa and subsequent progressive loss of supporting bone [1]. Peri-implantitis is a highly prevalent disease, with a mean patient prevalence of 22% [2].

The treatment of peri-implantitis is aimed to arrest the peri-implant inflammatory process and thus, to prevent further marginal bone loss [3]. In specific peri-implant lesions, regenerative therapies have also aimed to reconstruct the lost peri-implant bone [4]. Using these interventions, the biological feasibility of re-osseointegration has been documented in preclinical and clinical investigations [5–9], although the nature of the regenerated tissues is not well understood. Persson et al. [10] treated peri-implantitis lesions in dogs with a combination of systemic

Ignacio Sanz-Martín and Kyeongwon Paeng contributed equally to this work.

Summary: Thread geometry influenced the access of the decontamination devices and in turn its efficacy.

✉ Jae-Kook Cha
chajaekook@yuhs.ac

[1] Section of graduate Periodontology, Faculty of Odontology, Complutense University of Madrid, Madrid, Spain

[2] Department of Periodontology, Research Institute for Periodontal Regeneration, Yonsei University College of Dentistry, 50-1, Yonsei-ro, Seodaemun-gu, Seoul 120-752, South Korea

[3] ETEP (Etiology and Therapy of Periodontal Diseases) Research Group, University Complutense of Madrid, Madrid, Spain

antibiotics and surgical debridement using saline for decontaminating the implant surface. This approach failed to consistently achieve re-osseointegration. The authors concluded that re-osseointegration could only occur at sites where there was a pristine implant surface and that the presence of bacterial by-products leads to fibrous encapsulation.

In human clinical trials, in spite of the generally positive outcomes reported for reconstructive therapy of peri-implantitis defects, complications such as re-infections, implant loss or need of additional therapy have been reported after therapy [11–15].

In order to improve the predictability of the reconstructive approach in the treatment of peri-implantitis, different decontamination methods and devices have been tested in in vitro investigations. The outcomes of these investigations demonstrated the presence of residual biofilm after instrumentation [16–19]. This residual stain (biofilm) was mainly found in difficult to reach areas, such as between threads and in the thread surfaces facing downwards. This has suggested that implant-related characteristics, such as thread depth, thread pitch or thread design, could influence the outcome of decontamination procedures [20]. Recent investigations have already pointed out that implant features may influence the capability of the clinician to properly decontaminate the implant surface [20, 21]. Nonetheless, the impact of features such as thread depth, thread pitch or thread design is presently not well understood.

It was, therefore, the objective of this in vitro investigation to assess whether differences in the implant macro-geometry and thread pattern could influence the capability of three commonly used decontamination methods to access and debride the implant surface.

Material and methods

Study materials

Ninety-six implants from 4 different commercial brands were used ($n = 24$ per group) (Fig. 1a). Their thread design was evaluated with micro-CT and characterized by the following parameters: (i) thread depth (distance from the tip of the thread to the body of the implant), (ii) the thread pitch (the distance from the centre of the thread to the centre of the next thread), (iii) the thread shape (determined by the thread thickness and thread face angle including V-shape, buttress and reverse buttress) [22] and (iv) the upper and lower thread angle (both measured against a horizontal plane perpendicular to the long axis of the implant).

The characteristics of the four different implant groups were as follows:

- Group 1 ($n = 24$): Straumann Standard Tissue Level Implant RN (3.3 × 10 mm) (Straumann Institute, Basel, Switzerland) with a reverse buttress-thread shape (apically facing thread face is perpendicular to the implant axis and coronally facing thread is at a slant), thread pitch of 1.2 mm, thread depth of 0.3 mm, upper angle of 16° and a lower angle of 36°.
- Group 2 ($n = 24$): Dentium SimpleLine II 3.4 × 12 mm (Dentium, Suwon, South Korea) with a buttress-thread shape (coronally facing thread face is perpendicular to the implant axis and apically facing thread is at a slant), thread pitch of 0.6 mm, thread depth of 0.4 mm, upper angle of 9° and a lower angle of 26°.
- Group 3 ($n = 24$): Neobiotech IS III 3.5 × 10 mm (Neobiotech, Seoul, South Korea) with a buttress-thread shape, thread pitch of 0.75 mm, thread depth of 0.3 mm, upper angle of 14° and a lower angle of 37°.
- Group 4 ($n = 24$): Astratech Osseo speed TX 3.5S × 9 mm (Dentsply Implants, Mannheim, Germany) with a V-thread shape in the 2/3 apical of the implant and a micro-thread area in the coronal third. The micro-thread had a pitch of 0.2 mm, a depth of 0.07 mm and the upper and lower angles, 14° and 37°, respectively. In the V-threaded area, the pitch was 0.75 mm, the depth 0.3 mm and the upper and lower angles being 40° and 40°, respectively.

Implant staining

Test implants were submerged in a bath of a viscous water-resistant white ink (Winsor & Newton INK white Weiss, Winsor & Newton, London, UK) for 10 s, then air-dried with an air syringe in order to achieve an even dispersion of the stain over the implant surface [21]. Care was taken to avoid that the ink would access the implant connection or the transgingival components. Implants were then further dried at room temperature for 30 min and stored (Fig. 2a). In order to validate this staining methodology, 2 stained implants from each test group were evaluated by micro-CT analysis as a pilot (SkyScan 1072; SkyScan, Aartselaar, Belgium) with a resolution of 35 μm (at 100 kV and 100 μA) and visualized with 3D software (OnDemand3D; Cybermed, Seoul, South Korea). These 2 implants were not included in the sample size calculation and statistical analysis. The thickness of the ink layer (μm) was measured at 3 locations in each implant (coronal, middle and apical portion) at the thread valleys and in the 2 randomly selected aspects 180° apart on the implant platform.

Standardized defects

Custom-made circumferential defects were constructed around each implant using 3D printed models based on a previous in vitro study [16] (Fig. 2b). These models were designed using a dedicated software and a 3D printer with a resolution of 100 μ in grey resin material with a curing time of 15 min (Resin REF: FLGPWH04; FromLabs, Sommerville,

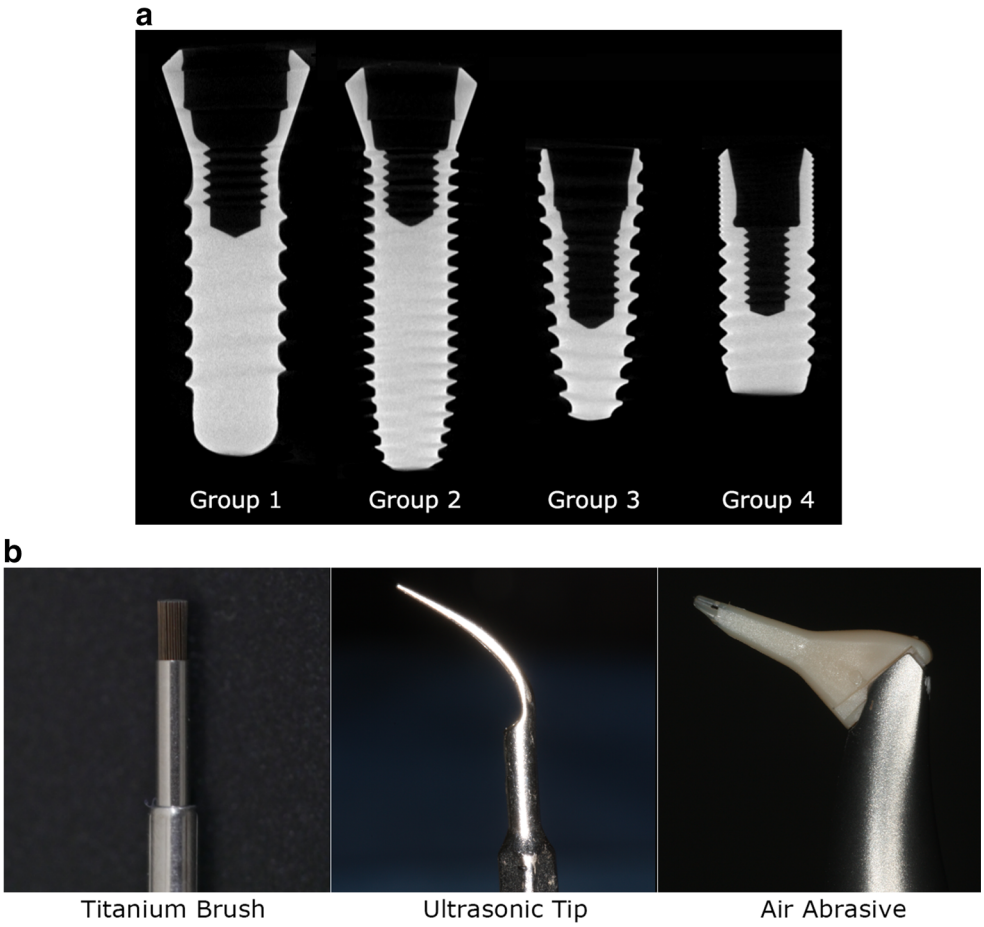

Fig. 1 **a** Micro-CT images of the different implant designs used in the investigation. Group 1 corresponds to Straumann Standard Tissue Level RN 3.3 × 10 mm, group 2 corresponds Dentium SimpleLine II 3.4 × 12 mm, group 3 corresponds to Neobiotech IS-III implant 3.5 × 10 mm and group 4 to Astratech Osseo speed TX 3.5S × 9 mm. **b** The different decontamination groups were TNB, TN-titanium brush; IST, ultrasonic tip of a cooper and silver alloy and PF, Perio-flow glycine-based air abrasive

MA, USA). The resulting models had a cubic shape with a circumferential defect in the centre and an access hole to insert implants leaving the most coronal 6 mm of its surface exposed. The dimensions of the circumferential defect were 6 mm in depth and 1.55 mm in width.

The stained implants were inserted in the resin models levelling the shoulder of the implant or the smooth-rough surface interface with the coronal border of the defect (Fig. 2c).

Decontamination protocols

Three decontamination groups of 32 implants per group were created. Each decontamination group had 4 subgroups of 8 implants based on the different implant designs. The in vitro design aimed to replicate the instrumentation of a circumferential defect by means of an open access flap surgery. The three decontamination groups were as follows (Fig. 1b):

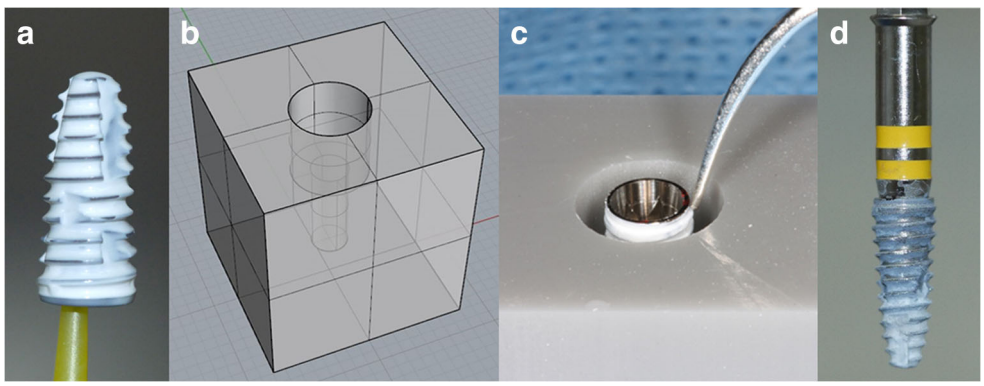

Fig. 2 **a** Implant coated with white ink. **b** 3D design of the defect configuration. **c** Implant inserted in defect and ultrasonic tip proceeding to instrumentation. **d** Implant removed from the printed defect after decontamination

1 TNB: Titanium implant brush made of titanium filaments within a tuft (TN Brush; Dentium) used with irrigation at 800 rpm and light pressure.
2 IST: Ultrasonic tip made of an alloy of copper and silver specially designed to minimize implant surface damage [23] (IS tip; B&L Biotech, Seoul, Korea) used under maximum irrigation and 80% power.
3 PF: A glycine-based air-powder abrasive device with a subgingival plastic nozzle (Perioflow; EMS, Nyon, Switzerland) used following the manufacturer recommendations, at maximum setting for both "liquid" and "power".

A calibration session with the use of the three mechanical decontamination methods was carried out before the start of the study to assure proper usage following the manufacturer guidelines. All tested implants were instrumented by a single experienced operator (ISM) during 120 s. Once completed, each implant was labelled with a permanent marker to identify the buccal area facing the operator and the left side of the implant.

Once removed from the printed defects (Fig. 2d) and rinsed with an air-water syringe to eliminate loosened particles, photographic images using a digital SLR camera (EOS 80D; Canon Inc., Tokyo, Japan) with 105 mm objective and a ring flash (Sigma, Sigma, Roedermark, Germany) were taken using standardized conditions (mode M, F32, 1/80, ISO 100) [16]. A custom-made splint was constructed to position the camera vertically to the implant axis (flat view) and with angulations of 60° (upper view) and 120° (lower view) to the implant long axis, respectively, thus allowing the assessment of the coronal and apical threads (Fig. 3a, b, c).

The obtained images were exported to the image analysis software (Adobe Photoshop CC; Adobe, San Jose, USA) and cropped to define an area of interest corresponding to the 6 mm of the surface left exposed in the defect.

The percentage of residual stain (PRS) was calculated using the following formula: area of residual stain × 100/ total area of implant surface (Fig. 4).

Scanning electron microscope analysis

The scanning electron microscope (SEM) evaluation in the area of the valley between threads was performed on the buccal aspect of the implants at the central level of the defect (approximately 3 mm from the implant shoulder) with a Zeiss Sigma 500 Microscope (Zeiss Microscopes, Zeiss, Oberkochen, Germany) using a magnification of × 500 with a working distance of 11.5 mm and operating at 5.00 KW.

Statistical analysis

Continuous variables were presented as means and standard deviations (SD). Normality of data distribution was tested by means of the Shapiro-Wilk test. The Kruskal-Wallis test was used to assess the differences between the decontamination groups and to analyse whether the implant design had an impact in the amount of residual stain. Dunn's post hoc test was used to check for pairwise comparisons between the three decontamination approaches and implant groups. These tests were performed using the SPSS software program (Version 20.0, IBM Corporation, New York, USA) with the statistical significance being set with an alpha level of 0.05.

The study was carried in compliance with the appropriate EQUATOR guidelines.

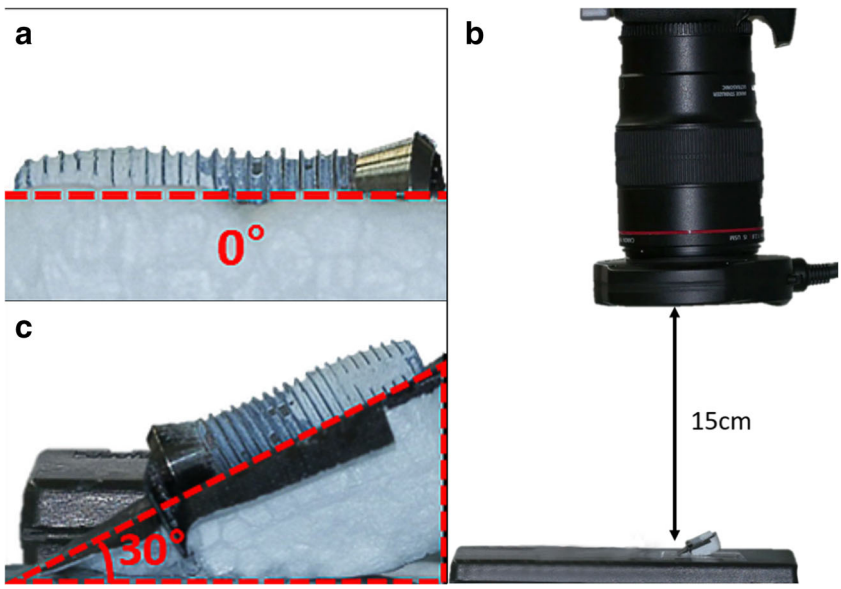

Fig. 3 **a** Installation of the implant for the flat view. **b** Camera settings and focal distance. **c** Installation of the implant for the lower view

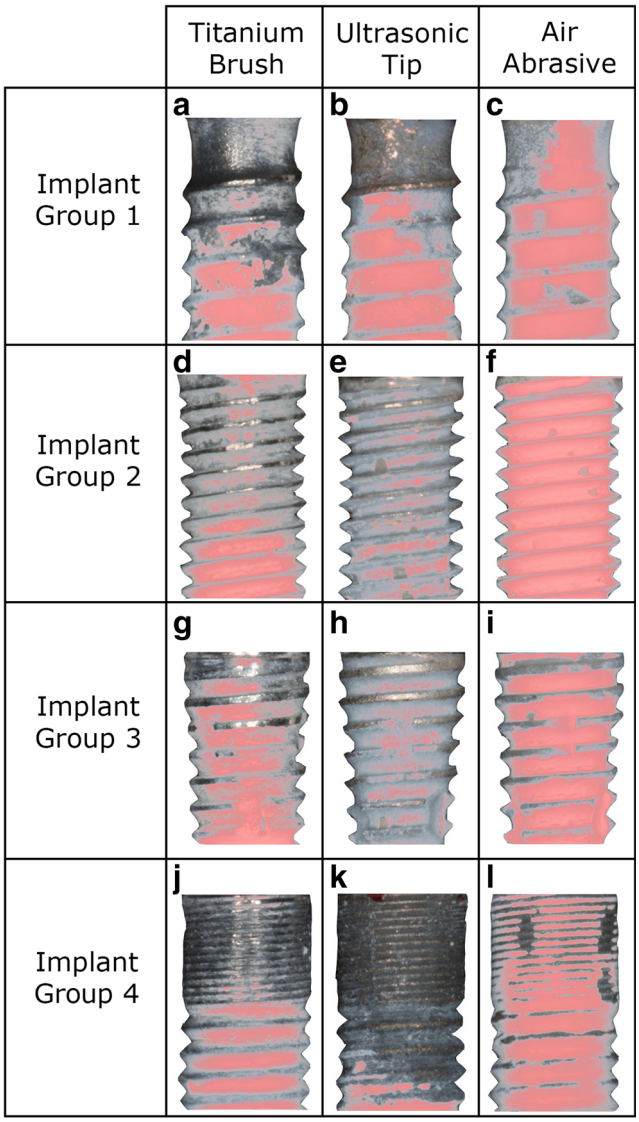

Fig. 4 Area of residual stain in red in the different implant designs and decontamination methods (the image corresponding to the median value has been selected)

Results

A total of 576 images, corresponding to 96 implants at the buccal and palatal sides using flat, upper and lower views, were analysed. This result section reports only the buccal sites. The results from the palatal sites are presented in Supplementary Table 1.

The validation of the staining methodology resulted in similar thickness of the ink layer for all the groups (mean thickness of 63.50 ± 6.02 μm, 63.42 ± 4.46 μm, 61.25 ± 5.21 μm and 62.50 ± 8.66 μm for test groups 1, 2, 3 and 4, respectively). Similarly, the total surface area (TSA) evaluated was similar for all the test groups (16.40 ± 1.41 mm^2, 17.50 ± 1.66 mm^2, 19.63 ± 2.3 mm^2 and 18.43 ± 2.13 mm^2 for groups 1, 2, 3 and 4, respectively).

Percentage of residual stain based on decontamination group and angle of evaluation

The results from the percentage of residual staining (PRS) after instrumentation with TNB are presented in Table 1 stratified by implant group and evaluation angle. In the flat view, the mean PRS by implant group were 34.56 ± 7.05, 27.78 ± 15.40, 47.57 ± 19.50 and 21.07 ± 12.95 for groups 1, 2, 3 and 4, respectively. Differences between groups were non-significant for the flat ($p = 0.078$), upper ($p = 0.699$) and lower views ($p = 0.094$). Differences in the PRS within each implant group based on the angles of evaluation were statistically significant for all the implant groups.

The results with the IST decontamination method are depicted in Table 1. In the flat view, the implant group 1 had a mean PRS of 37.43 ± 6.63, while in implant group 2, PRS was 27.34 ± 12.10; in implant group 3, 24.82 ± 16.17 and in implant group 4 11.93 ± 5.43. In this flat view, differences between groups were significant ($p = 0.004$). Also in the upper and lower views, differences were statistically significant ($p = 0.013$ and 0.008, respectively). When assessing pairwise comparisons, only the comparison between groups 1 and 4 reached significance ($p = 0.02$) in the flat view. Similarly, in the upper and lower view, only the comparison between groups 1 and 4 reached significance ($p = 0.007$ and $p = 0.006$ respectively). Finally, the differences in the PRS values based on the angles of evaluation within each implant group reached significance for all groups except for implant group 2.

The results with the PF decontamination method are depicted in Table 1. In the flat view, the mean PRS were 49.94 ± 6.78, 74.44 ± 6.21, 49.23 ± 7.81 and 47.51 ± 3.20 for groups 1, 2, 3 and 4, respectively. These differences between groups were statistically significant ($p = 0.01$). Also the PRS values in the upper and lower views demonstrated significant differences ($p = 0.035$ and 0.001, respectively). When evaluating the pairwise comparisons, in the flat view, differences between groups 1 and 2, groups 2 and 4 and groups 2 and 3 were statistically significant ($p = 0.02$, $p = 0.008$ and $p = 0.04$, respectively). On the upper view, none of the pairwise comparisons in PRS was significant, while in the lower view, only differences between groups 1 and 2 were significant ($p = 0.001$). The differences in the PRS values based on the angles of evaluation within each implant group reached significance for all groups.

Figure 5 depicts the PRS of the different groups based on the angle of evaluation and decontamination group.

SEM results

The effect of each decontamination method on the different implants is depicted in Fig. 6. All implant surfaces demonstrated residual stain in the form of subtle white shadows over the surface of the implant or clusters of ink debris along the

Table 1 Percentage of buccal residual staining for each decontamination method and implant group

a. Percentage of residual staining in TNB					
	Group 1	Group 2	Group 3	Group 4	p val (group)
Flat	34.56 ± 7.05	27.78 ± 15.40	47.57 ± 19.50	21.07 ± 12.95	0.078
Upper	38.48 ± 8.15	43.46 ± 13.44	39.09 ± 16.01	46.09 ± 18.10	0.699
Lower	50.23 ± 6.66	47.80 ± 14.16	63.65 ± 11.80	55.54 ± 16.94	0.094
p val (angle)	0.003	0.037	0.015	0.006	
Average	41.09 ± 9.75	39.67 ± 6.28	48.10 ± 19.06	40.89 ± 21.42	0.001
b. Percentage of residual staining in IST					
	Group 1	Group 2	Group 3	Group 4	p val (group)
Flat	37.43 ± 6.63	27.34 ± 12.10	24.82 ± 16.17	11.93 ± 5.43	0.004
Upper	50.00 ± 3.91	35.72 ± 19.86	38.70 ± 15.98	24.93 ± 11.16	0.013
Lower	56.73 ± 5.05	42.13 ± 10.18	45.18 ± 11.75	38.06 ± 9.68	0.008
p val (angle)	0.001	0.113	0.07	0.001	
Average	48.05 ± 9.62	35.06 ± 15.31	36.23 ± 16.72	24.97 ± 13.93	0.001
c. Percentage of residual staining in PF					
p val	Group 1	Group 2	Group 3	Group 4	p val (group)
Flat	49.94 ± 6.78	74.44 ± 6.21	49.23 ± 7.81	47.51 ± 3.20	0.01
Upper	58.47 ± 10.92	69.56 ± 10.25	60.80 ± 4.85	70.96 ± 9.29	0.035
Lower	69.43 ± 6.92	87.04 ± 1.96	78.38 ± 2.75	78.61 ± 5.03	0.001
p val (angle)	0.002	0.001	0.001	0.001	
Average	59.27 ± 11.45	77.01 ± 10.06	62.80 ± 13.33	65.69 ± 14.82	0.001

Implant group 1: Straumann Standard TL, implant group 2: Dentium Simple Line II, implant group 3: Neobiotech CMI implant and group 4 to Astratech Osseo speed TX

TNB TN-titanium brush; *IST* ultrasonic tip of a cooper and aluminium alloy; *PF* Perio-flow glycine-based air abrasive

implant surface. Layers of ink covering the implant surface at the valleys between threads were frequently found.

Discussion

The results of the present investigation showed that implant design had a distinct effect on the decontamination efficacy as evidenced by the differences encountered between the different implant groups; implants with lower thread pitch and thread depth values appeared to have a lower percentage of residual staining. Moreover, the decontamination group had also a significant influence on the decontamination outcomes with the air abrasives having the highest percentage of residual staining. The apically facing threads represented the most challenging areas to be accessed for all implant designs and decontamination methods.

The percentage of residual stain found in the present investigation is slightly higher than those reported in other investigations which found that narrow defects posed a greater challenge for decontamination devices and were frequently associated with residual stained areas [16, 24]. These differences between studies may, therefore, be attributed to (i) differences in the depth and width of the experimentally created defects, what resulted in areas with more or less difficulty of access and (ii) different methods of staining used in the in vitro experimental designs. The present investigation utilized a type of white ink highly adherent to the implant surface that only can be eliminated by mechanical disruption [21]. It is, therefore, possible that glycine particles used in the air abrasive device were not large enough to displace the ink from the implant surface.

It has been previously reported that air abrasives may have difficulties to remove calcified or well-adhered bacterial deposits [25]. Therefore in these situations, other options such as titanium brushes or ultrasonic tips may be preferable or needed as additional treatment. With ultrasonic devices, however, the efficacy of the ultrasonic tip vibration to effectively remove calcified deposits from the implant surface may be at the expense of creating surface alterations [26, 27]. Alternative options such as Teflon and plastic coatings have been found to leave frequent traces of the coating material remaining on the implant surface [28, 29]. In this investigation, we have used an ultrasonic tip made of an alloy (copper and silver) softer than titanium to minimize the damaging effect of the ultrasonic tip upon the implant surface [23].

The effect of the implant design was also notable. Implant group 4, which had the lowest thread pitch and depth values in its coronal aspect (micro-thread), obtained the lowest percentages of residual stain indicating that shallower threads were

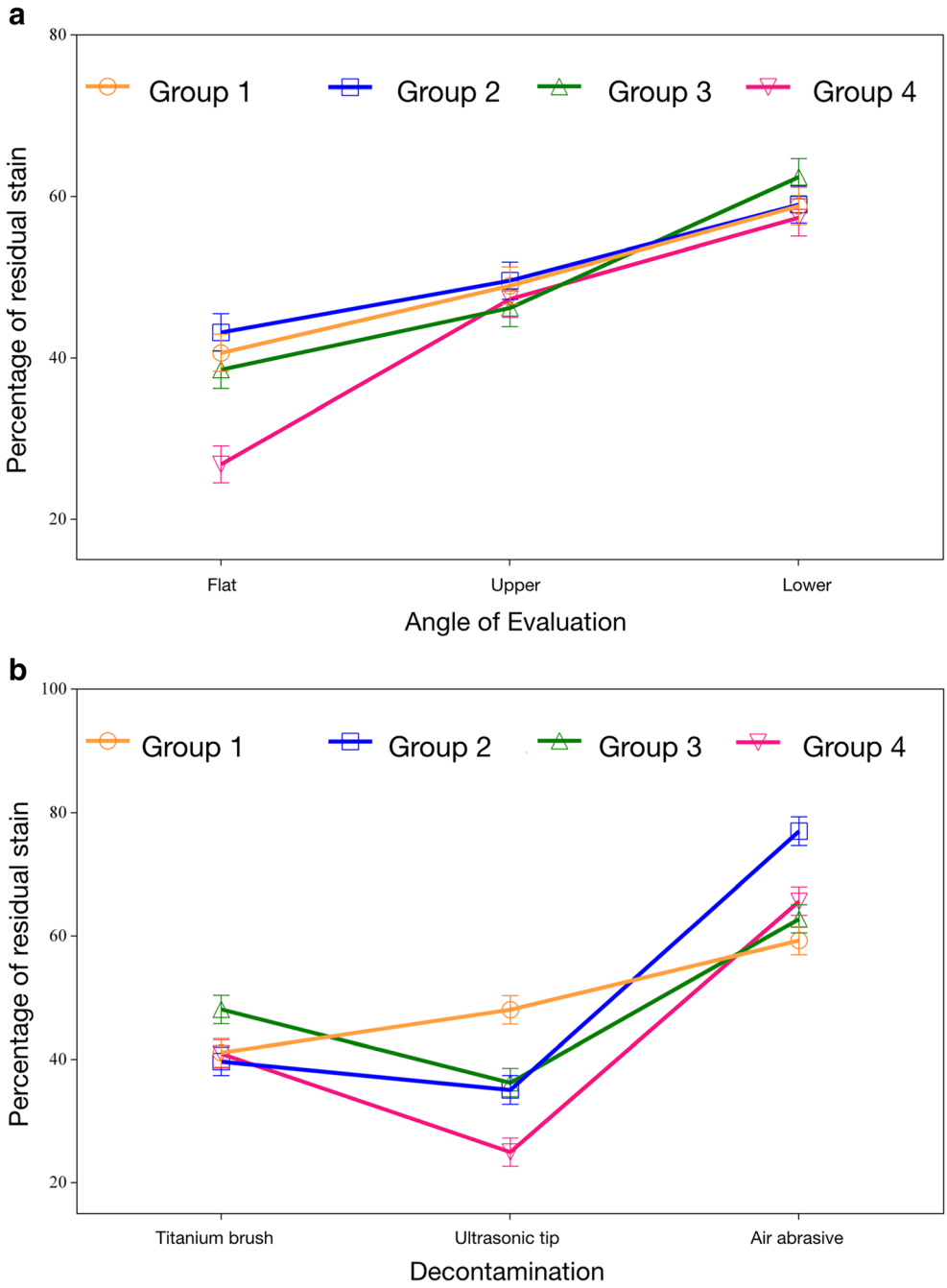

Fig. 5 **a** Percentage of residual staining of the different groups based on the angle of evaluation. **b** Percentage of residual staining of the different groups based on the decontamination group

easier to instrument. These results demonstrate that access to the surface is a significant factor for the efficacy of the mechanical decontamination method. Similarly, the design of the thread may also influence the efficacy since only the implant group 4 with the V-shape thread design demonstrated significantly less residual staining, while the other groups with buttress and reverse buttress designs showed a more limited access to the decontamination devices.

In group 1 and group 4 (group 1; without threads and group 4; with micro-threads in the coronal portion of the implant), the decontamination methods TNB and IST resulted in practically no residual staining in these areas where plaque is more likely to reside. On the contrary, when there was an increase in the depth of the defect (apical areas), or in the distance between threads, residual stain was more present, which underlines the importance of access for proper surface decontamination.

When ultrasonic instrumentation was used in implants with high thread pitch (group 1), the vibration applied on the tip of the thread was unable to remove the ink deposits at the thread valleys. However, in implants with narrower thread pitch, such as those in groups 2 and 3, ultrasonic instrumentation

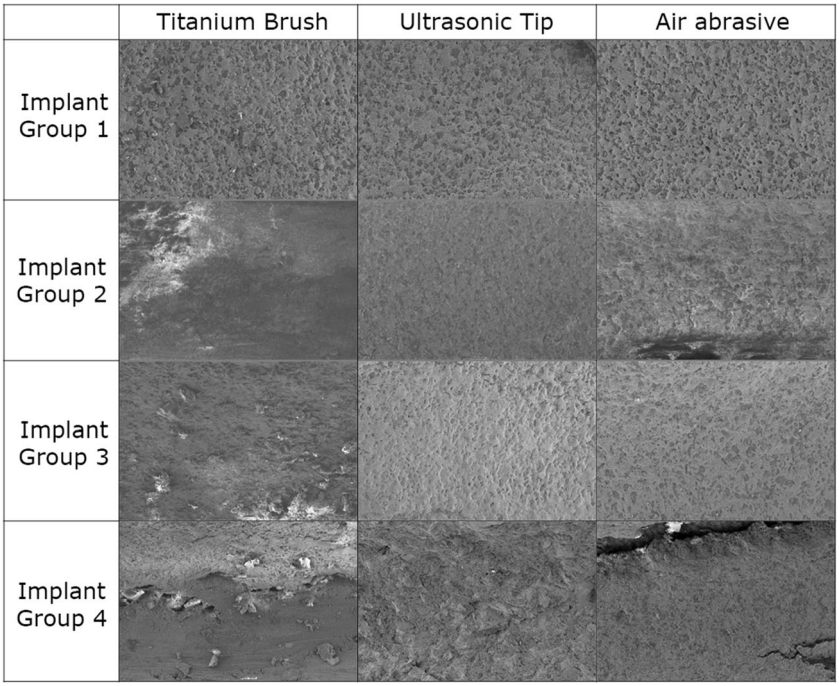

Fig. 6 SEM images of the valley areas after decontamination at a magnification of × 500

performed significantly better, showing that for this particular instrumentation protocol, the distance between threads may be more important than their depth.

With titanium brushes (TNB), the highest PRS were observed in group 3 with a marked buttress-thread design. This particular design may impede the access of the brush to the implant surface. In the buttress-thread design, the coronal facing thread has a flat design [30]; this flat thread was relatively easy to access but in contrast, it appeared to block the ability of the brush to reach the apically facing threads that had a slant and where the residual stain was significantly higher.

In order to extrapolate these results, it must be also acknowledged that all implants were instrumented without any abutments or reconstructions which facilitated the access to the decontamination devices.

The results of the present investigation must be interpreted with caution taking that it focused in only one step of the treatment of peri-implantitis and due to the nature of the in vitro design of the study and the use of ink as a surrogate to biofilm. Moreover, in spite of the similarities observed in ink-layer thickness, the implants utilized had different surfaces and this could have had an impact on the adherence of the surrogate biofilm.

Nevertheless, this investigation has provided information on the cleaning efficacy of three frequently utilized decontamination methods in four commercially available implant designs placed in standardized printed defects, using a validated staining method. Furthermore, these findings indicate the potential need of combining different decontamination methods (mechanical, chemical or biological) to maximize the biofilm and calculus removal.

Conclusions

Within the limits of this in vitro investigation, it can be concluded that considerable residual stain, particularly in the apical facing threads, was encountered in narrow deep defects after the use of three decontamination groups in all the implant designs tested. Thread geometry influenced the access of the decontamination devices and in turn its efficacy. Implants with lower thread pitch and thread depth values appeared to have less residual staining.

Supplementary Information The online version contains supplementary material available at https://doi.org/10.1007/s00784-020-03681-y.

Acknowledgements The authors would like to acknowledge the support of Prof. Ji-Man Park with the 3D printed models.

Author's contributions Ignacio Sanz-Martín: conception, design of the work, conduct of the experiment, data analysis and drafting the manuscript.
Kyeongwon Paeng: conduct of the experiment and data analysis.
Hyobin Park: conduct of the experiment and data analysis.
Jae-Kook Cha: conception, design of the work, conduct of the experiment, data analysis and support in manuscript writing.
Ui-Won Jung: critical revision of manuscript.
Mariano Sanz: critical revision of manuscript.

Funding This work was supported by the National Research Foundation of Korea (NRF) grant funded by the Korea government (MSIT) (No. NRF-2019R1C1C1006622).

Compliance with ethical standards

Conflict of interest The authors declare that they have no conflict of interest.

Ethical approval This article does not contain any studies with human participants or animals performed by any of the authors.

Informed consent For this type of study, formal consent is not required.

References

1. Berglundh T, Armitage G, Araujo MG, Avila-Ortiz G, Blanco J, Camargo PM, Chen S, Cochran D, Derks J, Figuero E, Hammerle CHF, Heitz-Mayfield LJA, Huynh-Ba G, Iacono V, Koo KT, Lambert F, McCauley L, Quirynen M, Renvert S, Salvi GE, Schwarz F, Tarnow D, Tomasi C, Wang HL, Zitzmann N (2018) Peri-implant diseases and conditions: consensus report of workgroup 4 of the 2017 World Workshop on the Classification of Periodontal and Peri-Implant Diseases and Conditions. J Periodontol 89(Suppl 1):S313–s318
2. Derks J, Tomasi C (2015) Peri-implant health and disease. A systematic review of current epidemiology. J Clin Periodontol 42(Suppl 16):S158–S171
3. Tomasi C, Regidor E, Ortiz-Vigon A, Derks J (2019) Efficacy of reconstructive surgical therapy at peri-implantitis-related bone defects. A systematic review and meta-analysis. J Clin Periodontol 46(Suppl 21):340–356
4. Faggion CM Jr, Chambrone L, Listl S, Tu YK (2013) Network meta-analysis for evaluating interventions in implant dentistry: the case of peri-implantitis treatment. Clin Implant Dent Relat Res 15(4):576–588
5. Carcuac O, Derks J, Abrahamsson I, Wennstrom JL, Petzold M, Berglundh T (2017) Surgical treatment of peri-implantitis: 3-year results from a randomized controlled clinical trial. J Clin Periodontol 44(12):1294–1303
6. Persson LG, Araujo MG, Berglundh T, Grondahl K, Lindhe J (1999) Resolution of peri-implantitis following treatment. An experimental study in the dog. Clin Oral Implants Res 10(3):195–203
7. Roccuzzo M, Pittoni D, Roccuzzo A, Charrier L, Dalmasso P (2017) Surgical treatment of peri-implantitis intrabony lesions by means of deproteinized bovine bone mineral with 10% collagen: 7-year-results. Clin Oral Implants Res 28(12):1577–1583
8. Schwarz F, Jepsen S, Herten M, Sager M, Rothamel D, Becker J (2006) Influence of different treatment approaches on non-submerged and submerged healing of ligature induced peri-implantitis lesions: an experimental study in dogs. J Clin Periodontol 33(8):584–595
9. Schwarz F, Claus C, Becker K (2017) Correlation between horizontal mucosal thickness and probing depths at healthy and diseased implant sites. Clin Oral Implants Res 28(9):1158–1163
10. Persson LG, Ericsson I, Berglundh T, Lindhe J (2001) Osseintegration following treatment of peri-implantitis and replacement of implant components. An experimental study in the dog. J Clin Periodontol 28(3):258–263
11. Schwarz F, Sculean A, Bieling K, Ferrari D, Rothamel D, Becker J (2008) Two-year clinical results following treatment of peri-implantitis lesions using a nanocrystalline hydroxyapatite or a natural bone mineral in combination with a collagen membrane. J Clin Periodontol 35(1):80–87
12. Schwarz F, Hegewald A, Sahm N, Becker J (2014) Long-term follow-up of simultaneous guided bone regeneration using native and cross-linked collagen membranes over 6 years. Clin Oral Implants Res 25(9):1010–1015
13. Roccuzzo M, Gaudioso L, Lungo M, Dalmasso P (2016) Surgical therapy of single peri-implantitis intrabony defects, by means of deproteinized bovine bone mineral with 10% collagen. J Clin Periodontol 43(3):311–318
14. Froum SJ, Froum SH, Rosen PS (2015) A regenerative approach to the successful treatment of peri-implantitis: a consecutive series of 170 implants in 100 patients with 2- to 10-year follow-up. Int J Periodontics Restorative Dent 35(6):857–863
15. Deppe H, Horch HH, Neff A (2007) Conventional versus CO2 laser-assisted treatment of peri-implant defects with the concomitant use of pure-phase beta-tricalcium phosphate: a 5-year clinical report. Int J Oral Maxillofac Implants 22(1):79–86
16. Sahrmann P, Ronay V, Sener B, Jung RE, Attin T, Schmidlin PR (2013) Cleaning potential of glycine air-flow application in an in vitro peri-implantitis model. Clin Oral Implants Res 24(6):666–670
17. Sahrmann P, Ronay V, Hofer D, Attin T, Jung RE, Schmidlin PR (2015) In vitro cleaning potential of three different implant debridement methods. Clin Oral Implants Res 26(3):314–319
18. Ronay V, Merlini A, Attin T, Schmidlin PR, Sahrmann P (2017) In vitro cleaning potential of three implant debridement methods. Simulation of the non-surgical approach. Clin Oral Implants Res 28(2):151–155
19. Charalampakis G, Ramberg P, Dahlen G, Berglundh T, Abrahamsson I (2015) Effect of cleansing of biofilm formed on titanium discs. Clin Oral Implants Res 26(8):931–936
20. Steiger-Ronay V, Merlini A, Wiedemeier DB, Schmidlin PR, Attin T, Sahrmann P (2017) Location of unaccessible implant surface areas during debridement in simulated peri-implantitis therapy. BMC Oral Health 17(1):137
21. Polak D, Maayan E, Chackartchi T (2017) The impact of implant design, defect size, and type of superstructure on the accessibility of nonsurgical and surgical approaches for the treatment of peri-implantitis. Int J Oral Maxillofac Implants 32(2):356–362
22. Abuhussein H, Pagni G, Rebaudi A, Wang HL (2010) The effect of thread pattern upon implant osseointegration. Clin Oral Implants Res 21(2):129–136
23. Unursaikhan O, Lee JS, Cha JK, Park JC, Jung UW, Kim CS, Cho KS, Choi SH (2012) Comparative evaluation of roughness of titanium surfaces treated by different hygiene instruments. J Periodontal Implant Sci 42(3):88–94
24. Keim D, Nickles K, Dannewitz B, Ratka C, Eickholz P, Petsos H (2019) In vitro efficacy of three different implant surface decontamination methods in three different defect configurations. Clin Oral Implants Res 30(6):550–558
25. Laleman I, Cortellini S, De Winter S, Rodriguez Herrero E, Dekeyser C, Quirynen M, Teughels W (2017) Subgingival debridement: end point, methods and how often? Periodontol 75(1):189–204
26. Cha JK, Paeng K, Jung UW, Choi SH, Sanz M, Sanz-Martin I (2019) The effect of five mechanical instrumentation protocols on implant surface topography and roughness: a scanning electron microscope and confocal laser scanning microscope analysis. Clin Oral Implants Res 30(6):578–587
27. Mengel R, Buns CE, Mengel C, Flores-de-Jacoby L (1998) An in vitro study of the treatment of implant surfaces with different instruments. Int J Oral Maxillofac Implants 13(1):91–96
28. Mann M, Parmar D, Walmsley AD, Lea SC (2012) Effect of plastic-covered ultrasonic scalers on titanium implant surfaces. Clin Oral Implants Res 23(1):76–82
29. Ruhling A, Kocher T, Kreusch J, Plagmann HC (1994) Treatment of subgingival implant surfaces with Teflon-coated sonic and ultrasonic scaler tips and various implant curettes. An in vitro study. Clin Oral Implants Res 5(1):19–29
30. Boggan RS, Strong JT, Misch CE, Bidez MW (1999) Influence of hex geometry and prosthetic table width on static and fatigue strength of dental implants. J Prosthet Dent 82(4):436–440